УДК 531.391 : 519.254

An experimental exploration of the dynamical chaos' structures

A.I. Prygunov
Polytechnic Faculty of MSTU, Technical Mechanics Chair

Abstract. In the paper a new approach to experimental research of dynamic chaos' structure has been offered. By examples of signals' and images' analysis the basic varieties of the structures and interrelation between chaotic structures have been shown. Some analytical relations for the interpretation of chaotic structures' evolution have been received. The studied examples concern to oceanology, paleoclimatology, paleontology, nanotechnology and economics.

Аннотация. В работе предложен новый подход к экспериментальному исследованию структуры динамического хаоса. На примерах анализа сигналов и образов показаны основные виды структур и взаимосвязь между ними, получены аналитические соотношения для интерпретации эволюции хаотических структур. Рассмотренные примеры относятся к океанологии, палеоклиматологии, палеонтологии, нанотехнологии и к экономике.

Key words: non-linear dynamics, complex dynamical systems, structure of dynamical chaos
Ключевые слова: нелинейная динамика, сложные динамические системы, структура динамического хаоса

1. Introduction

One of the main concepts of the modern non-linear dynamics is the concept of dynamical chaos (*Argyris et al.*, 1994; *Alligood et al.*, 1996). In theory the dynamical chaos can be considered as non-regular behavior of the dynamical systems which are formulated by the fully determined simultaneous equations (determined chaos). The concept of determined chaos is not equivalent to the traditional concept of randomness. The determined chaos in the complex dynamic systems has inside structures (periodic structures or local domains with the predictably behavior), but randomness can not have such structures neither in time domain (signals) nor in space domain (images).

There are a lot of principles for determination of the systems evolution's type as chaotic or as random. Mainly the methods are based on investigation of the systems trajectories in a phase space: fractal dimension, trajectories' entropy and others. The correct trajectories we can easily receive for the fully determinate systems in theory only. A correct reconstruction of the phase trajectories from experimental data is a difficult task. An embedding procedure must be used for decision of the task (*Takens*, 1981). Unfortunately the correct values of the time delay and the embedding dimension must be estimated for using imbedding procedure. Both the procedure's parameters can not be received by formal algorithms; therefore analyst must have special skill for successful usage of imbedding.

The autocorrelation analysis can be used for estimation of the time delay (*Williams*, 1997). The temporal lag which corresponds to the first zero of the autocorrelation function can be considered as suitable time delay for the signal. But such time interval for the random processes (correlation time τ_C) can be considered as minimal time of the processes' predictability τ_P too. For the chaotic processes the processes' predictability time interval (predictability time τ_P) must be multiplied greater than correlation time τ_C. In the paper we have accepted two rules for the processes recognizing:

1. If $\tau_P \approx \tau_C$ then investigated process is the random process; (1)
2. If $\tau_P > n\tau_C$ then investigated process is the chaotic process. (2)

In rule (2) n is the natural number (n>3).

2. Definition of the predictability time

Usually the measure of forecast's quality is the mean square of the error $\eta = |y(t) - z(t)|$

$$\langle \eta^2 \rangle = \langle |y(t) - z(t)|^2 \rangle,$$

where $y(t)$ – the experimental data series; $z(t)$ – the forecast of the data series (*Kravtsov*, 1993). Additionally we can introduce the correlation measure of forecast's quality (determination function):

$$D(\tau) = \frac{\langle y^2 \rangle + \langle z^2 \rangle + \langle \eta^2 \rangle}{2\left(\langle y^2 \rangle \langle z^2 \rangle\right)^{1/2}}, \text{ where } \tau = t\text{-}t_0. \quad (3)$$

An important point is that with the assumption $z(t)=y(t+\tau)$ as result we have $D(\tau)\equiv K(\tau)$, here $K(\tau)$ – the autocorrelation function.

The typical graphs of function (3) are presented in Fig. 1. From left to right: autocorrelation function $K(\tau)$ and determination functions $D_1(\tau)$, $D_2(\tau)$ for two processes which have equal correlation time τ_C but differ predictability time τ_P. The first process is a random process by rule (1), the second process is a chaotic process by rule (2).

The predictability time depends on more factors such as noise of measuring $н$, non-regular fluctuations in system f, incompleteness of prediction's models ΔM. In symbolic form we can write

$$\tau_P = F(\nu, f, \Delta M).$$

We can simplify a problem if $\nu = 0$ (the noise of measuring is neglected) and if $\Delta M = 0$ (the invariant prediction model)

$$\tau_P = F(0, f, 0). \quad (4)$$

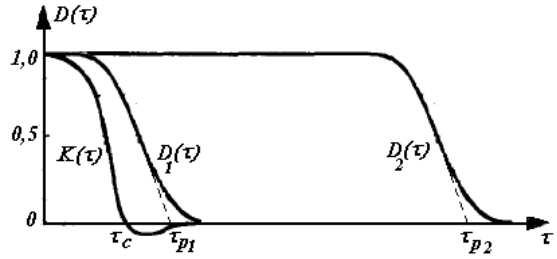

Fig. 1. The typical graphs of the determination function

In simple form (4) the predictability time depends on system's dynamics only. Usually systems have harmonical or quasi-harmonical dynamics therefore the harmonical or poly-harmonical prediction models can be used. For the harmonical or quasi-harmonical signals $\tau_C \approx T$, where T – the harmonical part's period, then the rules (1-2) must be rewritten:

1. If $\tau_P \approx T$ then investigated process is the random process; (5)
2. If $\tau_P > n\,T$ then investigated process is the chaotic process. (6)

Rules (5-6) require the preliminary analysis of investigated signals in time-frequency domain.

3. Time-frequency analysis for predictability time estimation

The basic procedures of signal's analysis are connected with signal's mappings from time domain in frequency domain (stationary signals) or in time-frequency domain (non-stationary signals). Mappings must be reversible as the process' energy must be an invariant of mapping. At choosing the harmonical prediction model searching the long-term harmonic components in signal will be needed irrespective of the component's magnitude.

For investigation of the dynamical chaos we offer a special method of time-frequency analysis (form-analysis) based on the wavelet-like time-frequency analysis with high resolution in the time domain and in the frequency domain too (*Prygunov*, 2008). Contrary to existing methods we have estimated not a power of spectrum, but a likeness of a signal's waveform to the waveform of pure harmonic (sinusoid) with any frequency from the analysis frequencies' set.

We can calculate the form-index for all allowed frequencies at any samples of the signal in digital form. Then the manifold of form-indexes is the two-dimensional matrix $\boldsymbol{I}_f(m,j)$, where m – the natural number which corresponds to harmonic's period T via samples' rate; j – the natural number which corresponds to the number of the sample at the digital representation of the signal. The values of the array cells belong to the real interval [-1,3]. The two-dimensional matrix $\boldsymbol{I}_f(m,j)$ we named a form-spectrum of signal.

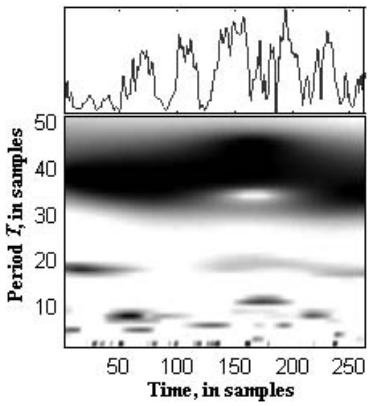

Fig. 2. The typical form-spectrum of the non-stationary signal (top – signal; bottom – form-spectrum)

The rules for estimation of predictability time via form-spectrum:

1. If we observe in the matrix an extensive (long-term) row of the cells with positive value, then we have a layer-like basin of process' predictability; (7)
2. An estimation of the basin's size along time axis can be accepted as predictability time. (8)

An example of application of rules (7-8) to estimation of predictability time we will present now.

The typical form-spectrum of the non-stationary signal is presented in Fig. 2. In accordance with the rule (7) the form-spectrum includes two layer-like basin of predictability with periods $T_1 \approx 40$ samples (main basin) and $T_2 \approx 20$ samples. At smaller periods (high-frequency fluctuations) we can observe only the small dark spots with irregular position. In accordance with rule (8) the predictability time $\tau_{P1} \approx 260$ samples (more than 6 T_1), the predictability time $\tau_{P2} \approx 180$ samples (about 9 T_2). As a result the quasi-periodic investigated process has chaotic low-frequency dynamics and random high-frequency dynamics.

4. The structure of dynamical chaos

There are three well-known ways for a chaotization in the dynamical systems: firstly, Feigenbaum's scenario via period's doubling; secondly, a dip to chaos via the alterations; thirdly, the chaotization in circle mapping via quasi-periodic dynamics' crushing (*Feigenbaum*, 1978; *Kuznetsov*, 2006; *Feudel et al.*, 2006). Our investigations of the chaotic structures show that the structures of dynamical chaos are genetically specified. But there are only two types of the chaos structure. The frequent type is Feigenbaum's structure which will be evinced in form-spectrum as series of period's doubling. The infrequent type is Fibonacci structure, which can be considered in theory as result of circle mapping in domain of "gold mean point" (GM), will be manifested in form-spectrum as Fibonacci series of the significant periods. We will show below that the last-named type of structure often can be considered as result of the first-named type's evolution.

In Fig. 3 the fundamental types of the dynamical chaos structures are presented. The chaotization by Feigenbaum's scenario via period's doubling is presented in Fig. 3a. It is the form-spectrum for the modeling signal which was received as digital solution of the Duffing's equation $x'' + kx' + x^3 = B\cos t$, where $k = 0{,}25$; $B = 8{,}86$. Till 300 samples the quasi-periodic oscillations there are. For the oscillations the main period equals 6,28 and period of the third sub-harmonic is equal 19 (in samples). In the initial stage of chaotization the fourth sub-harmonic 25 has appeared. Afterwards the periods 50 and 100 have appeared too as results of period doubling.

The chaotization via circle mapping is presented in Fig. 3b. The investigated signal was received from the circle map in form of iterative loop $x_{n+1} = x_n + r - (k/2\pi)\sin(2\pi x_n)$ (mod1) with "gold mean" parameters $(k,r)_{GM} = (1, 0{,}6067\ldots)$ for mapping (*Kuznetsov*, 2006). The periods of the oscillations which have appeared in this case (4, 7, 11, 19, 32) formed the Fibonacci series. An important point is that the Fibonacci series was formed in full only in second half of the spectrum as a result of the Feigenbaum's structure evolution which is presented in the initial part of the spectrum.

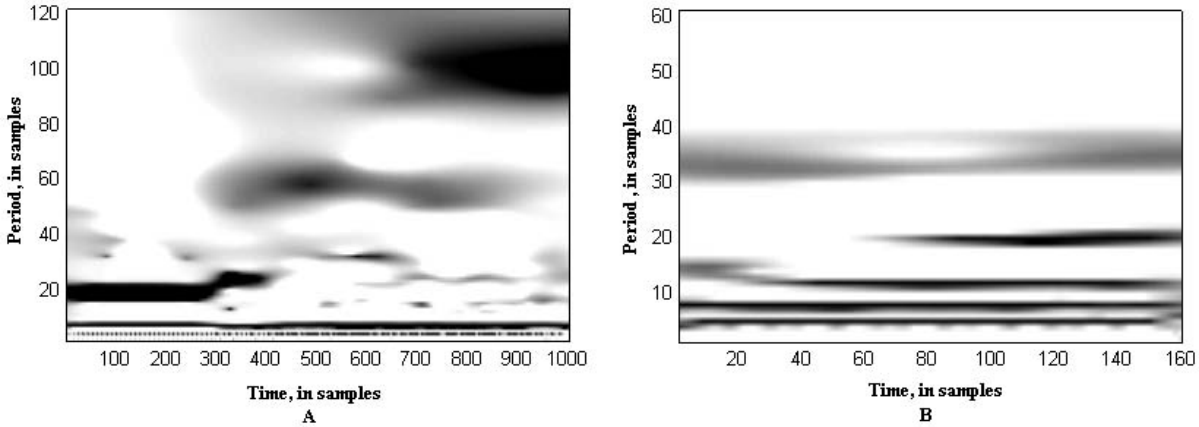

Fig. 3. The fundamental types of the dynamical chaos structures: a – Feigenbaum's structure (period doubling); b – Fibonacci structure (circle map in domain of gold mean point)

5. Temporal evolution of the chaotic structures (signals)

Below we will discuss some examples of the temporal evolution of the chaotic signals generated in the complex dynamical systems.

5.1. Trading chaos

The world markets (money-market, stock market and commodities market) can be considered as complex non-linear dynamical systems with dimension higher than 5 (*Shubik, Smith*, 2009), therefore the trading signals mainly are chaotic signals. A practice of the market's technical analysis partially confirms this assertion by the well known methods of the Fibonacci series' analysis.

The typical trading signals are presented in Fig. 4. The Australian dollar rate (Fig. 4a) has Fibonacci-like time-frequency structure (for comparison Fibonacci series 13, 21, 34, 55, 89 is presented in Fig. 4a). For such signals technical analysis (forecasting) via Fibonacci series can be successful. The rice's prices show period's doubling in time-frequency domain (Fig. 4b) (for comparison period doubling series 10, 20, 40, 80 is presented in Fig. 4b too). The signal is clearly predictable. In the left part of the picture there is the descending sine-like wave with periods about 20,40 trade days, in the right part there is the ascending sine-like wave with periods about 40,80 trade days. From the point of view of the predictability the Fibonacci chaos is deeper than Feigenbaum's chaos. But Fibonacci chaos in the trading signals is most common than Feigenbaum's chaos. The examined variants of the trading chaos' structure are not unique.

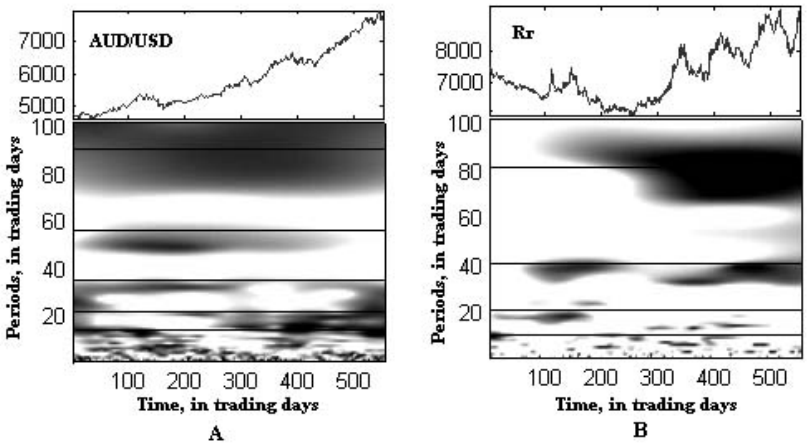

Fig. 4. The structures of trading chaos: a – Australian dollar rate AUD/USD (Fibonacci structure); b – rice's prices Rr (Feigenbaum's structure)

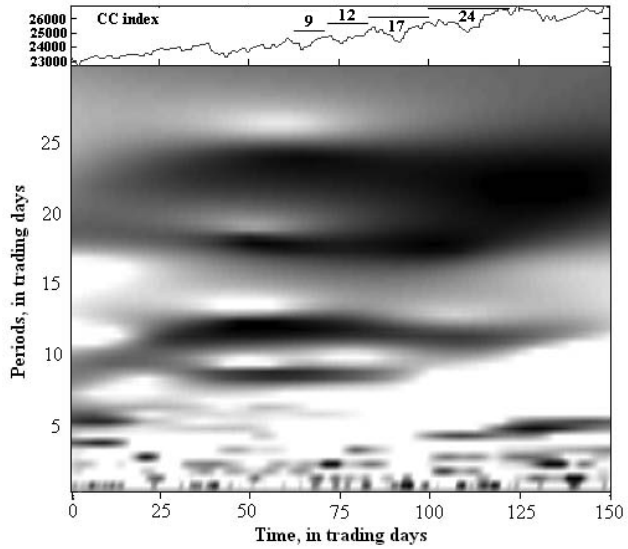

Fig. 5. The example of trading chaos' evolution: commodities composite index (CC – index)

In Fig. 5 the example of trading chaos' evolution is presented. The base structure in Fig. 5 is period's doubling: two layers with periods 10 and 20 trade days. But each layer bifurcates during the evolution. The periods after a bifurcation can be calculated: $T_H \approx 0{,}86T$; $T_L \approx 1{,}19T$, where T – the base period; T_H – the high-frequency period; T_L – the low-frequency period. Period 10 has bifurcated to periods $T_H \approx 9$; $T_L \approx 12$, period 20 – to periods $T_H \approx 17$; $T_L \approx 24$. The periods as the time intervals are presented in the top part of Fig. 5. The periods appear in the signal not simultaneously but as series with period's growing. It is clear that periods for forecasting will be $T_H \approx 35$; $T_L \approx 48$. An important point is that in form-spectrum all periods are presented already in a first third of the time scale before visible appearing of the periods in signal. It confirms the high sensitivity of the method to the dynamical structures' alterations even in an initial stage.

5.2. Climatic chaos

The global climate is multidimensional non-linear open system with chaotic behavior of the basic parameters such as temperature, atmospheric pressure, wind velocity and other. The problem of the climatic changes has a special significance in connection with the global warming problem. In Fig. 6 the global temperature's evolution according to the content of deuterium in Antarctic depth ice during 400 kyr (one kyr is one thousand years) is presented (*Petit et al.*, 1999). The two basic types of chaotic structure are presented in the picture. For ice with age greater than

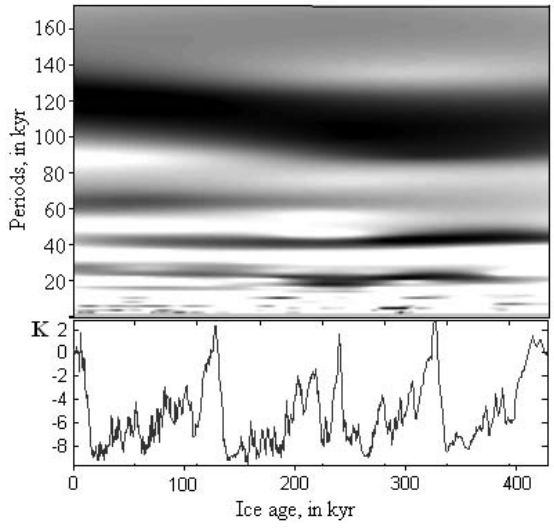

Fig. 6. The global temperature's evolution according to the content of deuterium in Antarctic depth ice during 400 kyr

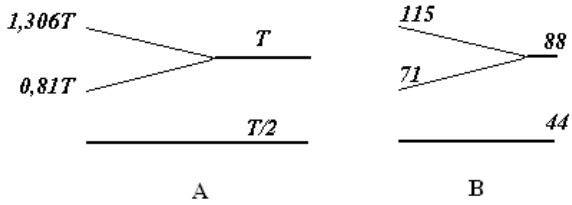

Fig. 7. The way of the period doubling structure's evolution to Fibonacci series: a – general theoretical estimation; b – application to Fig. 6

270 kyr the period's doubling structure (22 kyr, 44 kyr, 88 kyr) are observed. After 270 kyr the period's doubling structure began the evolution to Fibonacci-like structure (17 kyr, 27 kyr, 44 kyr, 71 kyr, 115 kyr).

In Fig. 7 the way of the period's doubling structure's evolution to Fibonacci series is presented. Here a direction of the process' development is from right to left. By general theoretical estimation (Fig. 7a) the period T must divide to periods $T_H \approx 0{,}81T$ and $T_L \approx 1{,}306T$ which will generate the Fibonacci series with sub-harmonic $0{,}5T$ ($0{,}5T$, $0{,}81T$, $1{,}306T$). An increase of the low-frequency period's duration and a depression of high-frequency periods in Fibonacci series can be plausible reason for the last glacial epochs. But high-frequency periods (17 kyr, 27 kyr) can determine the duration of the current interglacial period.

The global temperature's estimation according to the content of isotope O^{18} in marine microfossils during 1800 kyr (*Lisietski, Raymo*, 2005) are presented in Fig. 8. Three types of structures can be recognized in the picture. Before 1200 years ago period's doubling structure with periods 44 kyr (main period), 88 kyr, 176 kyr is presented. Between 1200 kyr and 700 kyr it was the random structure without main period. After 700 kyr the period's doubling structure with periods 44 kyr, 88 kyr (main period) is presented. The main period 88 kyr has developed to Fibonacci series with main period 115 kyr via bifurcation (see Fig. 7). After beginning of the bifurcation of the period 88 kyr (270 year ago) the conditions for the periodical glacier expansion were formed.

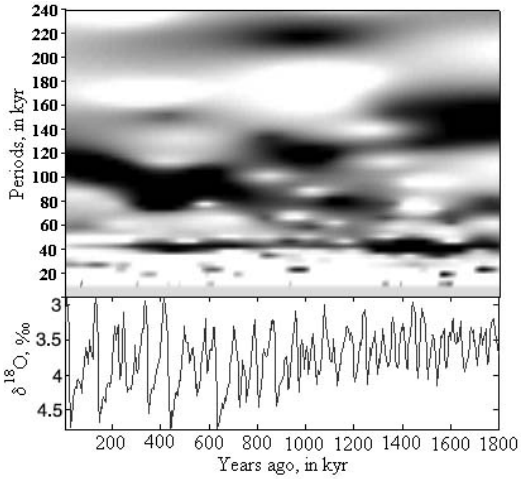

Fig. 8. The global temperature's estimation by content of isotope O^{18} in marine microfossils during 1800 kyr

5.3. Biotic chaos

Recently the fresh data for biota's diversity during Phanerozoe (about 600 millions years (Myr)) became available for investigation. In Fig. 9 the diversity curve for the sea invertebrate biota (SIB) (raw data) is presented. The curve shows that genera's extinction and genera's origination were periodic or cyclic. There are some hypotheses for such periods' explanation (cosmic year, Nemesis planet, global geophysical perturbation and other). In latest papers two main periods were established: 62 Myr and 27 Myr (*Alroy*, 2008; *Melott, Bambach*, 2010).

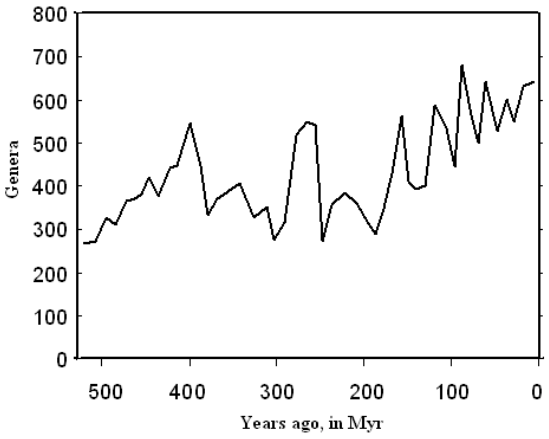

Fig. 9. The diversity curve for the sea invertebrate biota (SIB) (raw data)

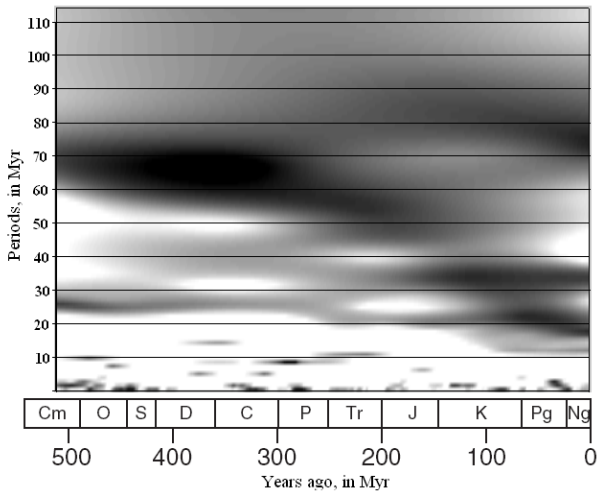

Fig. 10. Dynamics of the sea invertebrate biota's diversity during Phanerozoe

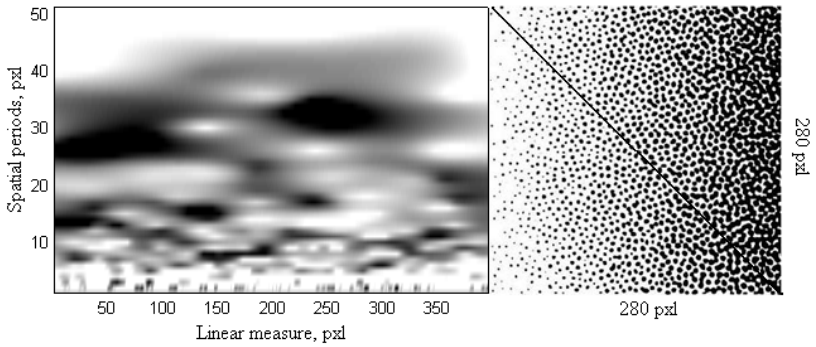

Fig. 11. Results of the form-analysis of the stochastic raster image

In Fig. 10 the results of diversity curve's form-analysis are presented. The picture shows two Fibonacci-like chaotic structures: before Permian 27 Myr, 43 Myr, 70 Myr (main period 70 Myr), after Permian 22 Myr, 35 Myr, 56 Myr, 91 Myr (main periods 22 Myr, 35 Myr). Second Fibonacci series of the periods is a result of first Fibonacci series' bifurcation by rule (see Fig. 7a) $T_H \approx 0{,}81T$ and $T_L \approx 1{,}306T$. Thus the dynamics of the sea invertebrate biota's diversity during Phanerozoe had only one great perturbation on a boundary between Permian and Triassic (about 250Myr ago), the fluctuations of the diversity became faster. The perturbation's time corresponds to period of the extreme trap volcanism in Siberia. The eruption of the Siberian Traps is considered to be a possible cause of the "Great Dying" (*Kuzmichev, Pease*, 2007). The early established periods 62 Myr and 27 Myr can be consider only as the mean values of the real low-frequency and high-frequency periods of the diversity curve. It is important to note, that the results are received on the basis of raw data's analysis without data's pretreatment (detrending and smoothing).

6. Spatial evolution of the chaotic structures (images)

There are chaotic structures not only in time domain as signals, but also in spatial domains (surfaces, volumes) as images. Below we will discuss some examples of spatial distribution of chaotic images.

6.1. Stochastic raster image

First of all we shall study the image with random spatial structure. As an example of such image we can consider random FM-screening, which is used at digital printing (image is available on www.tmk.ru/articles/images97/3.jpg).

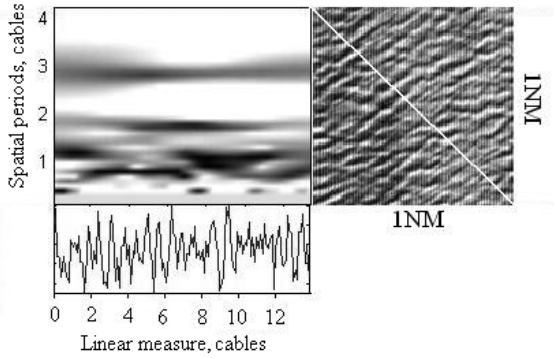

Fig. 12. Spatial distribution of sea waves

In Fig. 11 the results of the form-analysis of the stochastic raster image are presented. The form-analysis of the raster structure was carried out for image's diagonal (solid line). The form-spectrum includes the separated dark spots located in the irregular positions. The spot's width does not exceed three spatial periods thus by rules (2), (6) the investigated image has random structure. The disordered links between spots produce a foam-like structure.

6.2. Sea waves

From the point of view of an ordinary observer sea surface waves look like periodic structures. But sea surface can be considered as boundary between two poly-dimensional non-lineal dynamical systems: atmosphere and ocean, therefore sea surface waves mainly are quasi-periodic or chaotic structures.

In Fig. 12 spatial distribution of sea waves by satellite data for Bay of Bengal is presented (data is available on http://asterweb.jpl.nasa.gov/gallery/images/waves.jpg). Analyzed sea surface was about 1 square nautical mile (NM). The form-analysis of the waves' structure was carried out for image's diagonal (white line). The sea waves' structure shows Fibonacci-like series of spatial periods: 0,7; 1,0; 1,7; 2,7 nautical cables (NC = 0,1NM). The basic period of Fibonacci series (0,7 NC) is presented on spatial interval: (2-7) NC or 8 spatial periods, thus by rule (6) we have here a chaotic structure.

6.3. Nanostructures

Usually a nanostructure's forming happens as a spontaneous process in special conditions of an environment, therefore a process of the forming can be considered as a self-organization of nanoparticles. Thus the nanostructures must have a spatial structure. For identification of the spatial structure's presence in the nanostructures the form-analysis can be used.

In Fig. 13 two nanostructures are presented (images are available on http://www.nanometer.ru/2009/03/13/glina_esem_120059.html; http://www.nanometer.ru/2009/11/19/nanomateriali_nanochastici_158881.html).

Structure "worm" is typical for nanostructures of one-dimensional particles (nanowhiskers); structure "mosaic parquet" is typical for nanostructures of metals (nanofilms). The form-analysis of spatial structure was carried out for image's diagonals (white lines). The top structure shows period's doubling: 5 мм, 10 мм, 20 мм. The bottom structure shows Fibonacci-like series of spatial periods: 11 нм, 18 нм, 30 нм, 48 нм, 78 нм on the first half of picture and period's doubling: 22 нм, 44 нм, 88 нм on the second half of the picture. Both structures are chaotic, but not random. It is a distinctive feature of nanostructures, which can be used at diagnostics of nanostructures.

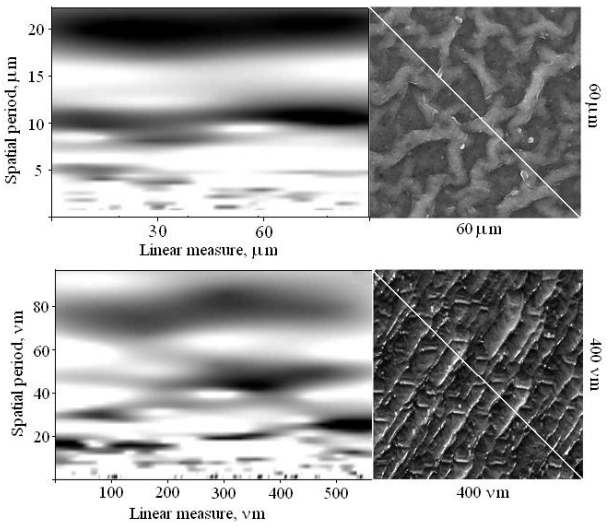

Fig. 13. Nanostructures: top – structure "worm"; bottom – structure "mosaic parquet"

7. Conclusions

For recognition of chaotic structures as distinct from random structures in the signals or images which are generated in complex dynamical systems the predictability time can be used. For estimation of the predictability time the form-analysis of signals or images can be applied. There are two basic varieties of the chaotic structures: period's doubling structures and structures with periods which correspond with Fibonacci series. Evolution of the chaotic structures can be considered as a result of the structures' changes via occurrence of the transition structures. The evolution can be both within one structural variety and with transition in other structural variety. The offered approach has a fundamental nature and can be used in a wide field of knowledge.

Acknowledgments. The author expresses gratitude to Prof. Adrian L. Mellot (University of Kansas, USA) for giving newest data about SIB diversity.

References

Argyris J., Faust G., Haase M. An exploration of chaos. An introduction for natural scientist and engineers. (Texts on computational mechanics.) *North Holland*, 750 p., 1994.

Alligood K.T., Sauer T.D., Yorke J.A. Chaos: An introduction to dynamical systems. (Textbooks in mathematical sciences.) *N.Y., Springer-Verlag*, 603 p., 1996.

Alroy J. Dynamics of origination and extinction in the marine fossil record. *PNAS*, v.105, p.11536-11542, 2008.

Feigenbaum M.J. Quantitative universality for a class of nonlinear transformations. *J. Stat. Phys.*, v.19, p.25-52, 1978.

Feudel U., Kuznetsov S., Pikovsky A. Strange nonchaotic attractors. Dynamics between order and chaos in quasiperiodically forced systems. *World Scientific, Singapore*, 228 p., 2006.

Kravtsov Yu.A. Fundamental and practical limits of predictability. *In: Limits of Predictability / Ed. Yu.A. Kravtsov. Berlin, Heidelberg, Springer-Verlag*, p.173-449, 1993.

Kuzmichev A.B., Pease V.L. Siberian trap magmatism on the New Siberian Islands: Constraints for Arctic Mesozoic plate tectonic reconstructions. *Journal of the Geological Society*, v.164, Iss. 5, p.959-968, 2007.

Kuznetsov S.P. Dynamical chaos. *Physmathlit, Moscow*, 356 p., 2006 (in Russian).

Lisietski L.E., Raymo M.E. A Pliocene-Pleistocene stack of 57 globally distributed benthic $\delta^{18}O$ records. *Paleoceanography*, v.20, PA 1003, doi: 10.1029/2004PA001071, 2005.

Melott A.L., Bambach R.K. Nemesis reconsidered. *Notices of the Royal Astronomical Society: Letters*, v.407, Iss. 1, p.99L-102L, 2010.

Petit J.R., Jouzel J., Raynaud D., Barkov N.I., Barnola J.M., Basile I., Bender M., Chappellaz J., Davis J., Delaygue G., Delmotte M., Kotlyakov V.M., Legrand M., Lipenkov V., Lorius C., Pйpin L., Ritz C., Saltzman E., Stievenard M. Climate and atmospheric history of the past 420,000 years from the Vostok Ice Core, Antarctica. *Nature*, N 399, p.429-436, 1999.

Prygunov A.I. A new tool for experimental investigation of chaos: Theory and applications. *Proceedings of the MSTU*, v.11, N 3, p.379-384, 2008.

Shubik M., Smith E. Building theories of economic process. *Complexity*, N 14, p.77-92, 2009.

Takens F. Detecting strange attractors in turbulence. *Lect. Notes in Math., Berlin, Springer*, N 898, p.336-381, 1981.

Williams G.P. Chaos theory tamed. *Washington, D.C., Joseph Henry Press*, 406 p., 1997.